Structural and electronic properties of the Bi/GaP(110) interface

M. Prietsch,* A. Samsavar, and R. Ludeke
IBM Thomas J. Watson Research Center, P.O. Box 218, Yorktown Heights, New York 10598
(Received 15 November 1990)

A systematic investigation of Bi on *n*-type GaP(110) with scanning tunneling microscopy (STM), scanning tunneling spectroscopy (STS), and ballistic-electron-emission microscopy (BEEM) is presented. The first 3 Å of Bi grows in a quasiordered monolayer, forming alternating chain and vacancy segments along the Ga-P zigzag chains with a periodicity of about 23 Å, which is consistent with the observed 6×1 low-energy electron diffraction (LEED) pattern. Additional Bi atoms aggregate to form $\simeq$10-Å-high clusters, which suggests a Stranski-Krastanov growth mode. The STS results show that the Bi monolayer is semiconductorlike with a band gap of about 0.55 eV; in contrast, the clusters exhibit metallic character. A 50-Å Bi film exhibited monocrystalline and atomically flat regions $\simeq$1000 Å in extent, which are delineated from similar adjacent regions by height differences equal to a biatomic step. LEED shows an ordered, two-domain hexagonal surface structure that consists of a close-packed-hexagonal arrangement of Bi atoms, as observed by STM. BEEM reveals a uniform Schottky-barrier height of 1.11 ± 0.02 eV at all measured positions across the sample surface.

I. INTRODUCTION

The structural and electronic properties of semiconductor interfaces have been of interest for decades.[1] With the development of scanning tunneling microscopy (STM) an important tool has been added to the arsenal of techniques for the study of these systems. STM allows not only a look at surface structure on an atomic scale in real space, but may also be used in a scanning tunneling spectroscopy (STS) mode that reveals important information about the spatially resolved electronic structure of surfaces. The latter technique is particularly advantageous for semiconductors, for which the study of band gaps as a function of location provided new insight into the origin of band bending.[2–4] Recently, another STM based technique, ballistic-electron emission microscopy (BEEM) has been developed for the spatially resolved investigation of the electronic properties of semiconductor interfaces buried $\simeq$100 Å below the sample surface.[5]

The adsorption of the group-V elements Sb and Bi on (110) surfaces of III-V semiconductors has been extensively studied in recent years because of their tendency to form ordered structures at the monolayer level.[2–4,6–15] These layers were perceived as prototypes for the study of structural and electronic properties of two-dimensional ordered layers. Such layers are also amenable to relatively simple structural[12,13] and band-structural[7,9] calculations. However, only Sb/GaAs[2] and Bi/GaAs[3,4] have been investigated on a microscopic scale, the former indicating the expected structural perfection at a monolayer, the latter clearly showing a defect structure consisting of missing Bi atoms, nearly periodically spaced, along the chainlike surface arrangement of the Bi atoms. A gap state in the semiconductorlike Bi monolayer was attributed to the missing Bi atoms.[4] The origin of the defect structure was attributed to misfit strain between the Bi and the GaAs. If correct, such strain would be even more dominant on a substrate with a smaller lattice constant, such as GaP(110). The results presented in this paper support the notion of a strain-induced defect structure. Hence, these adlayers are suitable as well for the study of structural defects in quasi-two-dimensional systems, in particular the role of defects on the electronic properties.

We present here STM, STS, and BEEM investigations of the Bi/GaP(110) interface with a recently developed microscope. In the monolayer regime, Bi grows on GaP(110) in a similar way as on GaAs(110).[3,4] Bi forms a quasiordered layer on the substrate that consists of short segments of Bi atoms in a chainlike arrangement followed by vacancies, the sequence repeating itself after about 6 unit cells in the [110] surface direction of the underlying GaP. STS reveals an $\simeq$0.55-eV-wide band gap of the film, compared to 0.7 eV for GaAs(110).[3,4] After completion of this layer additional Bi atoms form clusters that exhibit metallic character. Although we did not study the coverage regime necessary for cluster coalescence, the observed growth morphology suggests a Stranski-Krastanov growth mode. At higher coverages (50 Å) an atomically smooth Bi surface was observed, which exhibit a two-domain structure of hexagonal symmetry. BEEM reveals a Schottky-barrier height of 1.11 ± 0.02 eV, a value which was found to be uniform across the sample surface.

II. EXPERIMENTAL DETAILS

The experiments were performed in an UHV system consisting of a preparation/analysis chamber with a LEED facility, and a separate STM chamber. Both chambers are pumped with combinations of ion pumps

and Ti sublimation pumps, resulting in a typical base pressure of $\simeq 7\times 10^{-11}$ mbar.

The entire STM assembly is supported by a two-stage string suspension with eddy-current damping. This combination, $\simeq 40$ cm in height, resulted in a resonance frequency of $\simeq 1$ Hz for the lower stage, on which the STM is mounted. The tubular piezoelectric element used for scanning the tunneling tip is mounted on a sled that rests on polished sapphire tracks. The sled, held in position solely by friction, is pushed in a horizontal direction (z) by a Burleigh Inchworm® for coarse approach. The approach, under computer control, consists of alternating Inchworm steps and axial (z) extensions of the piezoelectric scanner until tunneling is achieved. Subsequently, the Inchworm and sled are decoupled by reversing the Inchworm, a procedure that prevents Inchworm-induced drifts and vibrations. The lateral sample position (x and y) can be coarsely adjusted by two retractable, *in situ* screwdrivers. Extensive use of materials like machinable ceramic (Macor™) and Ti, which exhibit thermal expansion coefficients similar to that of the piezoelectric ceramic, reduce thermal drift velocities to $\simeq 1-5$ Å/min. The design allows *in situ* manipulations such as UHV sample transfers between chambers, tip changes, and tip cleaning by electron-beam heating. The tips are electrolytically etched from a 0.25-mm diameter W wire that is spot-welded on a 2.5-mm diameter tip holders. Up to four of these holders can be loaded into the chamber for tip replacements. The lateral and vertical excursions at the tip position of the piezoelectric scanner have been calibrated using a stepped Si(111)7×7 surface. The measured heights (z) have an uncertainty of $\simeq 5\%$, while lateral (x and y) distances have somewhat larger uncertainties of $\simeq 10\%$ that are mainly due to variations in lengths between different tips. In addition, thermal drift may lead to sheared images, and may also increase the error in the y direction.

For BEEM measurements, contact to the metal film is provided by a grounded gold-wire electrode that can be moved in two dimensions (x and z) by two cross-mounted Inchworms. The tunnel voltage is provided by the tip bias, and for BEEM measurements, the sample bias, which is nominally zero, may be adjusted to compensate for voltage offsets, as, for example, thermovoltages. It should be noted here that all viewports of the STM chamber have to be sealed against outside light to suppress photocurrents. Both tunnel current (at the tip) and BEEM current (at the sample) are amplified by operational amplifiers with gains of 0.1 and 1 V/nA, respectively; these are mounted inside the UHV in close proximity to tip and sample current sources. Particularly for spectroscopy, this arrangement is an essential measure to minimize pickup noise and ground-loop problems, and results in current noise of $\lesssim 1$ pA. Furthermore, proper electrical shielding of the Inchworms, the scanning element, and all high-voltage lines inside and outside the UHV was necessary to prevent pickup noise.

The microscope is driven by an STM control unit that is connected to an IBM PS/2 model 80 computer by parallel digital data lines. Optoisolators in these lines prevent ground-loop problems and high-frequency pickup noise from the computer. All conversions to and from analog signals are done inside the control unit, which further reduces noise. The STM control unit provides the analog signals to the high-voltage amplifiers for the scanner, bias voltages, and power to the preamplifiers inside the UHV chamber, input and output to the lock-in amplifier, and digital lines (again with optoisolators) to the Inchworm control unit. The tip position relative to the surface is controlled by a feedback circuit, which maintains a constant tunnel current. During spectroscopy this circuit may be switched off by computer-controlled analog switches, in order to keep the tip at a constant position, or to ramp the tip position relative to the sample (see below). Additional analog switches control the modulation of the tip voltage for lock-in measurements, and the axial (z) motion of the piezoelectric scanner during approach operations. 16-bit analog-to-digital converters read the current and the z position of the piezoelectric scanner, whereas its x and y positions are controlled by 16-bit digital-to-analog converters. Tip and sample bias voltages, tunnel current value, as well as ramp and approach voltages for the axial motion of the piezoelectric scanner are provided by 12-bit digital-to-analog converters.

STS and BEEM spectra may be taken either at a predefined grid of tip positions or at spontaneously chosen positions by hitting a "hot key." For STS, the feedback control for the z position of the tip is interrupted, and the tip current I is measured as a function of tip voltage V. To measure the derivative dI/dV, V is modulated by a 50-mV, 400-Hz, ac signal, and dI/dV is obtained from a lock-in amplifier. In later data analysis, the normalized differential conductivity $(dI/dV)/(I/V)$ is calculated, which shows the main features of the density of states of the sample.[16] One major advantage of this normalization procedure is the insensitivity to tip-position changes due to drift or glitches, which affect both I and dI/dV in the same way. The acquisition method further decreases the dynamic range of I and dI/dV by moving the tip toward the sample with decreasing tip voltage.[2] This procedure has been shown to improve the signal-to-noise ratio of $(dI/dV)/(I/V)$ at low tip voltages without changing the shape of the spectra. In our case, a ramp of 1 Å/V was used. Each STS spectrum takes about 10 sec.; low-pass filters with a time constant of 10 msec. were used to smooth out high-frequency components in I and dI/dV, which derive from both the random noise and the 400-Hz oscillations of the tip voltage. This time constant corresponds to an average voltage shift and spectral broadening of $\simeq 5$ meV, which is negligible compared to the $\simeq 50$-meV resolution limit due to the modulation. BEEM I-V spectra were taken by ramping the tip voltage under feedback control, thereby keeping the tunnel current constant. One BEEM spectrum takes about 30 sec., and a low-pass filter with a time constant of 100 msec was used to improve the signal-to-noise ratio, leading to negligible broadening and shifts of < 10 meV for BEEM spectra.

Clean (110) surfaces were obtained by cleavage of prenotched $4\times 4\times 10$ mm^3 single-crystal bars of n-type GaP (Te doped with 2×10^{17}/cm^3) using the knife-anvil

method. Bi was evaporated from a carefully outgassed quartz crucible, located $\simeq 200$ mm away from the sample, at a rate of 6–7 Å/min and a pressure of $\simeq 5\times 10^{-10}$ mbar. Evaporation rates were calibrated with a quartz microbalance. For BEEM measurements, a 50-Å-thick Bi dot, 2 mm in diameter, was evaporated through a mask placed in close proximity to the semiconductor surface. This measure reduces the interface area and prevents short circuits via the edges of the crystal, and results in a high zero-bias resistance of the Schottky diode (>10 MΩ), thereby achieving a low input noise of the current preamplifiers.

III. RESULTS AND DISCUSSION

A. Structure of a Bi monolayer

Figure 1 depicts a 1000-Å×750-Å STM image for $\simeq 3$ Å of Bi on GaP(110), together with contour profiles along selected lines. 3.39 Å represents the nominal value for a vacancy-free Bi monolayer of atomic density equal to that of the GaP(110) surface (9.52×10^{14} cm^{-2}). Within the shown grey-scale range of 12 Å, the surface appears flat, except for occasional Bi clusters that are $\simeq 200$ Å apart. The diameters of the clusters are estimated to be $\simeq 20$–50 Å, and their heights range from 7 to 15 Å. This results in a cluster size containing $\simeq 30$–300 Bi atoms. We did not observe atomic ordering on top of the clusters, which have rather smooth surfaces, probably because of the very close-packed arrangement of the Bi atoms. These clusters, as we will discuss later, appear to exhibit metallic character.

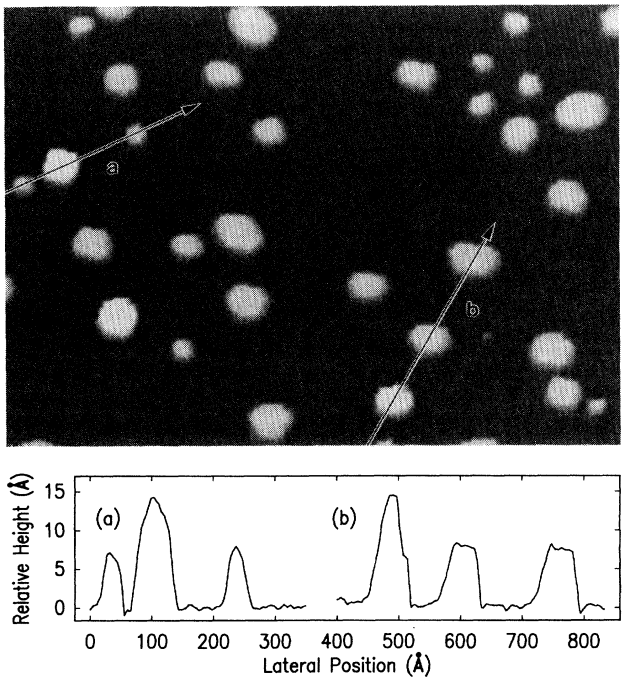

FIG. 1. Topographic image of a 1000-Å×750-Å-large surface area of 3.2 Å Bi on GaP(110), taken at a tip voltage of 2.5 eV with 1 nA tunnel current. The height range from black to white is 12 Å. Two contour profile plots along selected lines, indicated by arrows (a) and (b), are also shown.

In Fig. 2 we show a 100-Å×100-Å high-resolution image of the same sample in an area between the clusters. The Bi atoms form short chains of average length $\simeq 14$ Å oriented parallel to the [110] surface direction, which corresponds to that of the zigzag Ga-P chains of the GaP(110) surface. In the orthogonal [001] direction the Bi chains are separated from neighboring chains by $\simeq 5.4$ Å. The image of these chains consists of slightly elongated blobs separated by 4.1 ± 0.4 Å. This separation is slightly larger than the 3.85-Å length of the underlying unit cell of the GaP surface in the [110] direction, which contains one Ga and one P atom. The observed separation of the blobs is thus closer to that observed for Bi on GaAs(110) (with a unit cell width of 4.0 Å), for which two Bi atoms per unit cell have been identified.[3,4] Based on this similarity, as well as on the known coverage, we believe that each blob in Fig. 2 corresponds to two Bi atoms. Thus each chain segment consists of 6–8 Bi atoms, with both longer and shorter segments observed

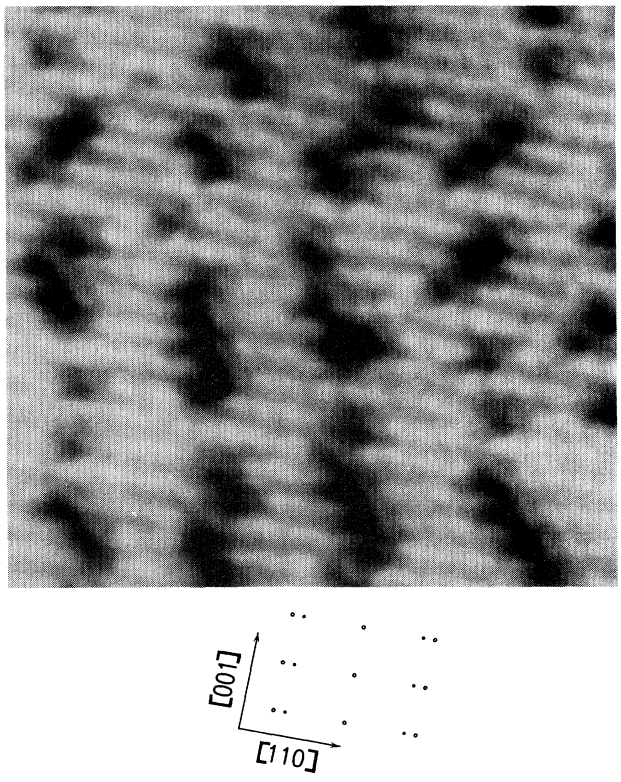

FIG. 2. Topographic image of 100-Å×100-Å surface area of 3.2 Å Bi on GaP(110) on a flat part of the surface, taken at a tip voltage of 2.1 eV and a tip current of 1 nA. Weak "ghosts," probably due to a two-atom tip, are observed at the edges of the vacancy areas. The image has not been corrected for thermal drift. The height range from black to white is 1 Å. A schematic plot of the respective LEED picture is also shown, the open dots representing the GaP(110) spots, and the solid ones those from the overlayer.

as well. The collinear Bi chain segments are separated by a vacancy region 8–12-Å wide, which corresponds to ≃4–6 missing Bi atoms. The average repeat distance in the [110] direction is ≃23 Å. Figure 2 clearly shows that the vacancy segments tend to align laterally to form domains that are typically 10–30-Å wide. A schematic plot of the LEED picture of this sample is also included in Fig. 2. The LEED pattern reveals additional spots due to the Bi overlayer in the [110] direction, which are $\frac{1}{6}$ of the reciprocal lattice constants away from the stronger spots assigned to clean GaP(110). With a lattice constant for GaP of 5.45 Å, this 6×1 pattern from the Bi overlayer then originates from a 5.45-Å×23.1-Å unit cell, a value which is in good agreement with the STM observations. This means that the Bi overlayer matches the GaP(110) surface lattice well in the [001] direction, and that the observed vacancy areas are on average 6 substrate lattice constants apart in the [110] direction.

We may now conclude that the first monolayer of Bi on GaP(110) forms a quasiordered epitaxial overlayer, with the Bi atoms arranged in similar geometric positions with respect to the substrate surface unit cell. The latter, in the [110] direction, has 2 atoms in a zigzag arrangement with a repeat distance of 3.85 Å. This value appears to be too short to accommodate long-range epitaxial Bi growth with a one-to-one correspondence between Bi and substrate atoms, since the typical nearest-neighbor distance for Bi is 3.11 Å in its rhombohedral structure (2.92 Å is a tetrahedral environment[17]). The observed separation of ≃4.1 Å per unit Bi cell implies that for Bi—Bi bond lengths of 2.92–3.11 Å, the Bi atoms would lie in a compressed zigzag arrangement with subtended angles between 82° and 89°. This range is somewhat less than the 86° to 100° range in rhombohedral Bi, the latter value corresponding to the bond angle among atoms of the shortest bond length (3.11 Å). Clearly, the match between overlayer and substrate is tenuous at best, with the strain of the mismatch resulting in short Bi chains. From the extent of the vacancy segment following each Bi chain segment, it appears that the induced strain requires several surface cell distances to relax. The aggregation or islanding of both Bi and vacancy regions, over which the strain is more evenly distributed, appears to minimize shear stresses, which would be considerable if segments of Bi chains and vacancies alternated in the [001] direction. The notion of strain as the source of the observed morphology is consistent with a recent structural investigation of the Bi/GaAs(110) system, which exhibits a similar 6×1 periodicity that consists of a more perfect chain structure of usually five unit cell distances (10 or 11 atoms) interrupted by a Bi vacancy.[3,4] The longer length of the chains can be attributed to the larger GaAs lattice constant of 4.00 Å in the [110] direction, which leaves more space for the Bi atoms along the chains.

B. STS results

Representative $(dI/dV)/(I/V)$ curves at different sample locations are shown in Fig. 3. Before we discuss the spectra in detail, we will describe the method used to calculate the ratio of the dI/dV and I/V spectra for

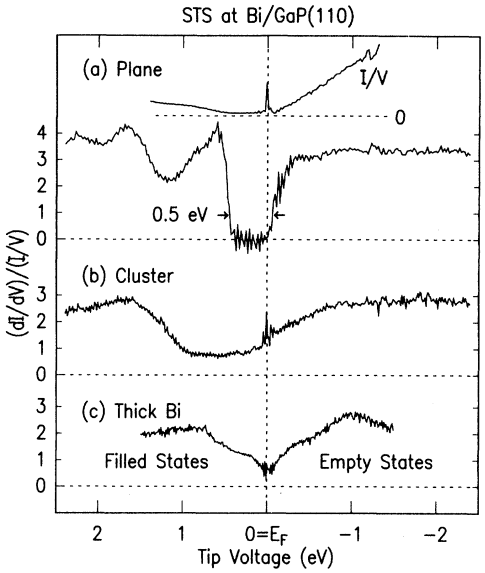

FIG. 3. $(dI/dV)/(I/V)$ curves derived from STS spectra taken at 3.2 Å Bi on GaP(110) in the plane (a), and on top of a cluster (b). For comparison, a spectrum of a thick Bi film is also shown (c). For spectrum (a) the value of I/V was modified to $\sqrt{(I/V)^2+c^2}$, as shown in the upper curve, to reduce noise in the band-gap region.

semiconductors. For these materials the tunnel current I, as well as dI/dV, are zero in the band-gap region, so that the ratio $(dI/dV)/(I/V)$ cannot be calculated directly from the measured spectra. However, $(dI/dV)/(I/V)$ should be zero in this region, since it represents the local density of states.[16] Several approaches have been taken to overcome this problem with the aim of not changing the information contained in the original data.[2] The approach usually taken sets I/V to finite values over the problematic range. One should note, however, that these methods change the relative weight of features observed in the $(dI/dV)/(I/V)$ spectra. Here, instead, we use a rather simple offset method: I/V is replaced by $\sqrt{(I/V)^2+c^2}$, where c is a small constant. This modification is negligible for $I/V \gg c$. However, c has to be chosen large enough so as not to accentuate the noise signal in the band-gap region, but not as large as to affect the spectral shape. The results of this procedure are shown in Fig. 3(a). The upper curve shows the I/V data after modification with $c=0.02$ nA/V. The offset is clearly observed in the zero-conductivity region around E_F. The lower curve shows the resulting $(dI/dV)/(I/V)$ data. It should be noted that variations of c do not affect the observed band gap, but change the relative heights of the features just outside the band-gap region. For curves (b) and (c), I/V was not modified. The I/V curves generally exhibit a glitch at $V \simeq 0$ that results from the division of a small voltage value into a generally finite, noise-derived value of the tunnel current [see Fig. 3(a), top spectrum]. This glitch may then lead to another one, but of opposite sense, in $(dI/dV)/(I/V)$ around 0 V, which is of relatively minor consequence, as observed

in curve (c). The offset of dI/dV, which is mainly due to phase misadjustment in the lock-in amplifier, is a more critical parameter for the spectral evaluation, in particular for semimetals. The phase, and hence the offset, can be properly adjusted either during tunneling in the band-gap region of a semiconducting part of the surface, or, alternatively, while retracting the tip out of tunneling.

We will now discuss the spectra in detail. Spectrum (a) is representative of those in the plane area, at least 50 Å away from a Bi cluster, and represents the density of states in the Bi monolayer. The spectrum exhibits an $\simeq 0.5$-eV wide gap, with the Fermi energy close to the conduction-band minimum. The actual size of the band gap of the Bi film may be up to 0.1 eV larger, since the 50-meV oscillator amplitude of the lock-in amplifier may reduce the energy resolution by a similar amount at each band edge. Thus we conclude that Bi forms a semiconducting layer on top of GaP(110) which exhibits a band gap of 0.55 ± 0.05 eV.

We did not observe significant variations of the spectra with location on the plane, except an $\simeq 0.1-0.2$-eV smaller band gap in the neighborhood of clusters (less than $\simeq 30$ Å away). This may be due to metallic states from the Bi clusters penetrating into the band gap of both the semiconducting Bi layer and the substrate.[18] The metal-induced gap states, well known from the Schottky-barrier theory, have a typical decay length of $\simeq 10$ Å in the semiconductor.[19,20] Thus they should be detectable in the neighborhood of clusters. Spectrum (b) for a cluster shows a finite density of states at the Fermi energy, which is typical for metals. Metallic behavior for Bi clusters is rather surprising, since Bi is a semimetal. This property is clearly indicated in spectrum (c) for an 80-Å-thick Bi film, which shows the characteristic dip in the density of states at the Fermi energy. In addition, small clusters of materials which are bulk metals are often nonmetallic up to rather large cluster sizes. The observed metallicity of the clusters is probably due to a different crystal structure of Bi in the clusters. However, we were not able to resolve atomic structure in the clusters.

We did not observe the Fermi-level position directly at the conduction-band minimum of the Bi layer, which would be expected for the n-type substrate used here. This may also be due to the presence of metallic clusters, which pin the Fermi level at a different position. We note here that the observed spectra in the plane are rather similar to those taken at the Bi/GaAs(110) system, which has a similar morphology and exhibits a 0.7-eV-wide band gap.[3,4]

C. Structure at 50 Å coverage

A large-area STM image of a 50-Å-thick Bi overlayer on GaP(110) is shown in Fig. 4, together with a contour profile plot. The surface consists of large, atomically flat areas of $\simeq 1000$-Å size. They are separated from each other by $\simeq 4$-Å-high steps, as seen from the contour profile. From the magnitude of the step it may be concluded that they are two atom layers high.

Two STM images of a smaller area, taken at different tip voltages, are shown in Fig. 5, together with a schematic plot of the respective LEED pattern. The LEED pattern exhibits a two-domain hexagonal structure, which is rotated by $\simeq \pm 5°$ with respect to the GaP(110) substrate pattern. We note that we could observe both the Bi and the substrate pattern at the same

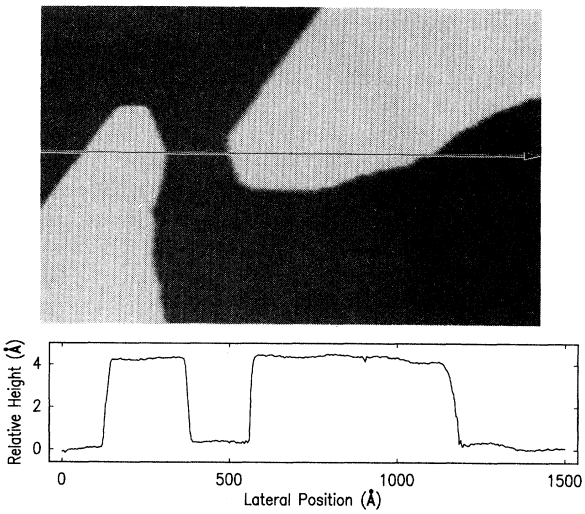

FIG. 4. Topographic image of a 1500-Å × 1000-Å area of a 50-Å-thick Bi film on GaP(110), together with a contour profile plot, indicated by an arrow. Tip voltage was −1 eV, tip current 0.2 nA. The grey-scale range is 6 Å.

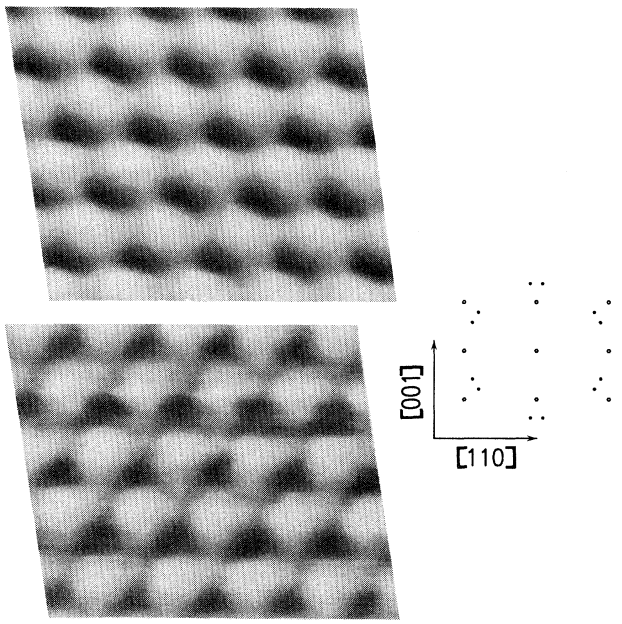

FIG. 5. Topographic images of a 20-Å × 17-Å area of a 50-Å-thick Bi film on GaP(110), at a tip current of 1 nA. Tip voltage is 0.5 eV for (a) and −1.0 eV for (b). The grey-scale range is 0.8 Å for (a) and 0.3 Å for (b). The images have been corrected for thermal drift. A schematic plot of the corresponding LEED picture is also shown, the open dots represent the substrate spots, and the solid dots come from the overlayer.

time with variable relative intensity by moving the electron beam from the Bi dot to the bare GaP surface and back. Since from LEED we know that the structure is hexagonal, we corrected the STM images in Fig. 5 to achieve this symmetry; the distortion in the image is due to thermal drift effects. In addition, the used drift velocities were confirmed by images taken at slower scanning speed. This leads to images showing a close-packed hexagonal structure, which a nearest-neighbor distance of 4.3 Å, in good agreement with 4.5±0.1 Å calculated from the LEED image, and also with the nearest-neighbor distance of 4.56 Å in the (111) plane of rhombohedral Bi. In the upper image, taken at 0.5 V tip bias, we observe that the deepest tip positions are not centered between three triangularly arranged atoms, but rather lie directly in between two atoms. On the other hand, the image taken at −1-V tip bias, at approximately the same position, reveals holes in the center of those three-atom triangles pointing down, but rather shallow areas at triangles pointing up. These voltage-dependent effects may be due to the spatial distribution of the respective Bi orbitals, which varies with energy. Effects of tip geometry may also play a role. The lower STM image may be explained through the arrangement of atoms in the second Bi layer, which fill only half of the triangles of the Bi(111) surface.

D. BEEM spectroscopy

The result of the BEEM experiment is shown in Fig. 6. We observed rather uniform spectra at different lateral positions of the tip, what is also expected for such a flat surface. The spectra were fitted with a thermally broadened $\frac{5}{2}$ power dependence around threshold.[21,22] The fits reveal a Schottky-barrier height of 1.11±0.02 eV, which is uniform at different lateral positions within the accuracy of our analysis ($\simeq$0.02 eV). However, we note that in some cases we observed thresholds with up to 0.3 eV larger values. These deviations are attributed to tip contamination or to Bi uptake of the tip during approach, leading to a nonmetallic coating of the tip. A strongly reduced tunneling probability from the electrons at the Fermi level of the tip then increases the observed voltage threshold.[21] These effects underline the importance of a clean UHV environment for BEEM studies using tip or metal-film materials which are sensitive to contamination.

IV. SUMMARY AND OUTLOOK

In summary, we have shown that Bi forms a quasiordered overlayer on GaP(110) in the monolayer regime,

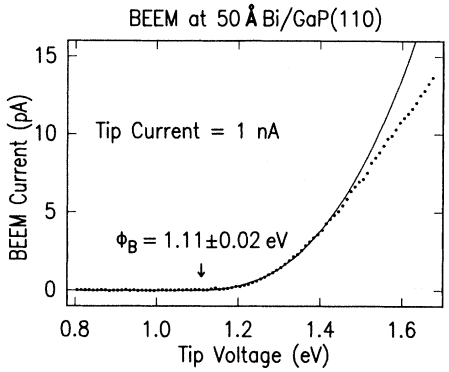

FIG. 6. Representative BEEM spectrum for a 50-Å-Bi film on *n*-type GaP(110), together with a fit (solid curve) with a thermally broadened $\frac{5}{2}$ power law.

with 6–8 atom long chains in the [110] direction. This is similar to the behavior of Bi on GaAs(110), where the chains are usually 10 or 11 atoms long. If we compare the nearest-neighbor distance in elemental Bi (3.09 Å) with the lattice constant in the [110] direction of GaP (3.85 Å) and GaAs (4.00 Å), we can relate the longer chains with less lattice strain. An investigation of Bi growth on even larger III-V semiconductors may therefore lead to an epitaxial monolayer. Good candidates for such an investigation are InAs and GaSb.

The Bi film on GaP is found to be semiconductorlike with a 0.55-eV-band gap, which is similar to the Bi/GaAs(110) system (0.7 eV). After completion of the first layer, metallic Bi clusters grow on top of this film. The origin of this fascinating result remains speculative at this time, although a detailed study of metallicity as a function of cluster size should contribute to a better understanding of its cause. For thick films (50 Å), a smooth hexagonally ordered surface with monoatomic steps was observed. Finally, BEEM measurements of the Schottky barrier height of Bi on *n*-type GaP(110) indicated uniform barrier heights across the sample of 1.11 eV.

ACKNOWLEDGMENTS

The authors thank the staff of IBM Yorktown, in particular M. Prikas, C. Candotti, F. Maurer, R. Kaufman, R. M. Feenstra, C. K. Shih, and M. Lutz for extensive help building the STM and assistance during the experiments.

*Permanent address: Institut für Experimentalphysik, Freie Universität Berlin, Arnimallee 14, D-1000 Berlin 33, Germany.

[1]E. H. Rhoderick and R. H. Williams, *Metal-Semiconductor Contacts* (Clarendon, Oxford, 1988).

[2]P. Mårtensson and R. M. Feenstra, Phys. Rev. B **39**, 7744 (1989).

[3]A. B. McLean, R. M. Feenstra, A. Taleb-Ibrahimi, and R. Ludeke, Phys. Rev. B **39**, 12 925 (1989).

[4]R. Ludeke, A. Taleb-Ibrahimi, R. M. Feenstra, and A. B. McLean, J. Vac. Sci. Technol. B **7**, 936 (1989).

[5]W. J. Kaiser and L. D. Bell, Phys. Rev. Lett. **60**, 1406 (1988).

[6]P. Skeath, C. Y. Su, W. A. Harrison, I. Lindau, and W. E. Spicer, Phys. Rev. B **27**, 6246 (1983).

[7]C. Mailhiot, C. B. Duke, and D. J. Chadi, Phys. Rev. Lett. **53**, 2114 (1984).
[8]F. Schäffler, R. Ludeke, A. Taleb-Ibrahimi, G. Hughes, and D. Rieger, Phys. Rev. B **36**, 1328 (1987).
[9]F. Manghi, C. Calandra, and E. Molinari, Surf. Sci. **184**, 449 (1987).
[10]J. J. Joyce, J. Anderson, M. M. Nelson, C. Yu, and G. J. Lapeyre, J. Vac. Sci. Technol. A **7**, 850 (1989).
[11]W. K. Ford, T. Guo, S. L. Lance, K. Wan, S.-L. Chang, C. B. Duke, and D. L. Lessor, J. Vac. Sci. Technol. B **8**, 940 (1990).
[12]J. P. LaFemina, C. B. Duke, and C. Mailhiot, J. Vac. Sci. Technol. B **8**, 888 (1990).
[13]M. Menon and R. E. Allen, J. Vac. Sci. Technol. B **8**, 900 (1990).
[14]A. Tulke, M. Mattern-Klosson, and H. Lüth, Solid State Commun. **59**, 303 (1986).
[15]N. Esser, M. Reckzügel, R. Srama, U. Resch, D. R. T. Zahn, W. Richter, C. Stephens, and M. Hünermann, J. Vac. Sci. Technol. B **8**, 680 (1990); C. Stephens, D. R. T. Zahn, K. Fives, R. Cimino, W. Braun, and I. T. McGovern, *ibid.* **8**, 674 (1990).
[16]N. D. Lang, Phys. Rev. B **34**, 5947 (1986).
[17]L. Pauling, *The Nature of the Chemical Bond,* 3rd ed. (Cornell University Press, New York, 1960).
[18]P. N. First, J. A. Stroscio, R. A. Dragoset, D. T. Pierce, and R. J. Celotta, Phys. Rev. Lett. **63**, 1416 (1989).
[19]C. Tejedor, F. Flores, and E. Louis, J. Phys. C **10**, 2163 (1977).
[20]J. Tersoff, Phys. Rev. Lett. **55**, 465 (1984).
[21]M. Prietsch and R. Ludeke, Surf. Sci. (to be published).
[22]M. Prietsch and R. Ludeke (unpublished).

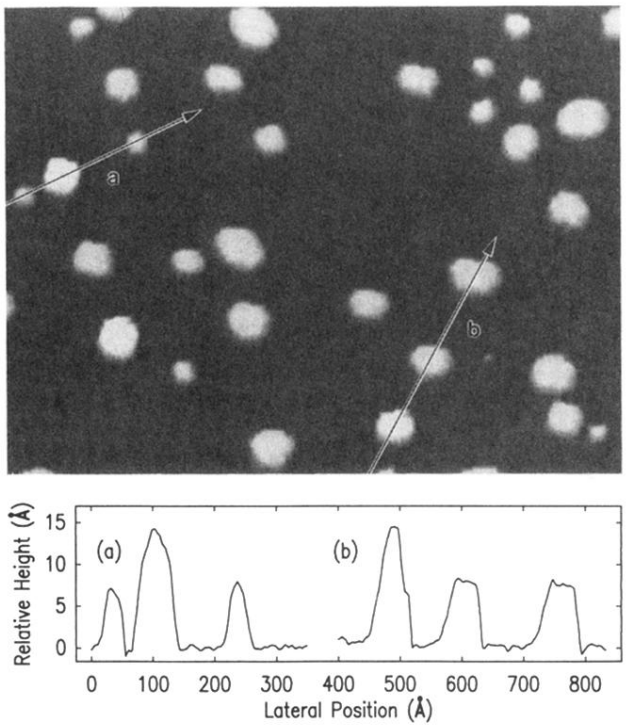

FIG. 1. Topographic image of a 1000-Å×750-Å-large surface area of 3.2 Å Bi on GaP(110), taken at a tip voltage of 2.5 eV with 1 nA tunnel current. The height range from black to white is 12 Å. Two contour profile plots along selected lines, indicated by arrows (a) and (b), are also shown.

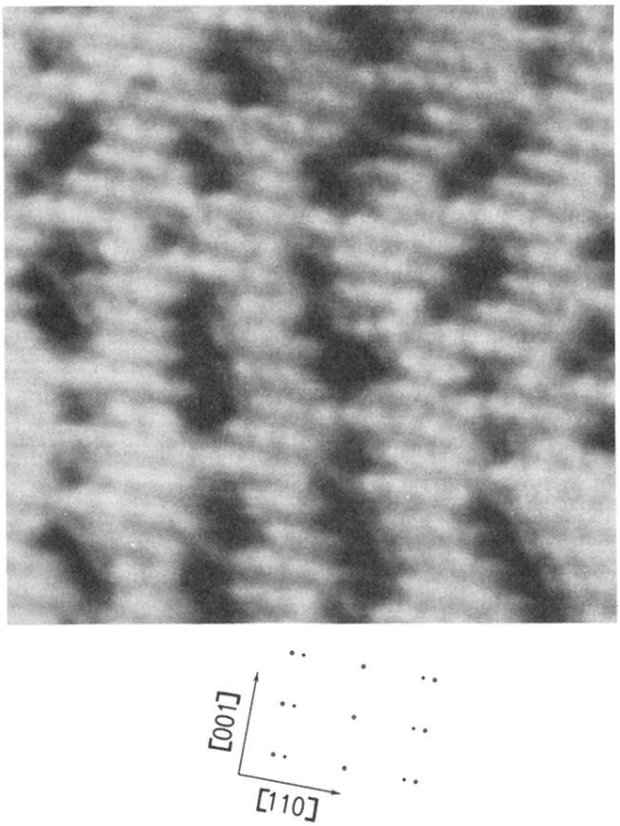

FIG. 2. Topographic image of 100-Å × 100-Å surface area of 3.2 Å Bi on GaP(110) on a flat part of the surface, taken at a tip voltage of 2.1 eV and a tip current of 1 nA. Weak "ghosts," probably due to a two-atom tip, are observed at the edges of the vacancy areas. The image has not been corrected for thermal drift. The height range from black to white is 1 Å. A schematic plot of the respective LEED picture is also shown, the open dots representing the GaP(110) spots, and the solid ones those from the overlayer.

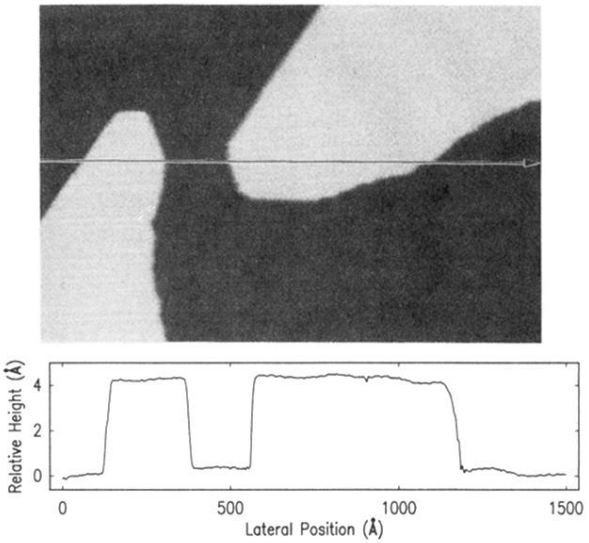

FIG. 4. Topographic image of a 1500-Å × 1000-Å area of a 50-Å-thick Bi film on GaP(110), together with a contour profile plot, indicated by an arrow. Tip voltage was −1 eV, tip current 0.2 nA. The grey-scale range is 6 Å.

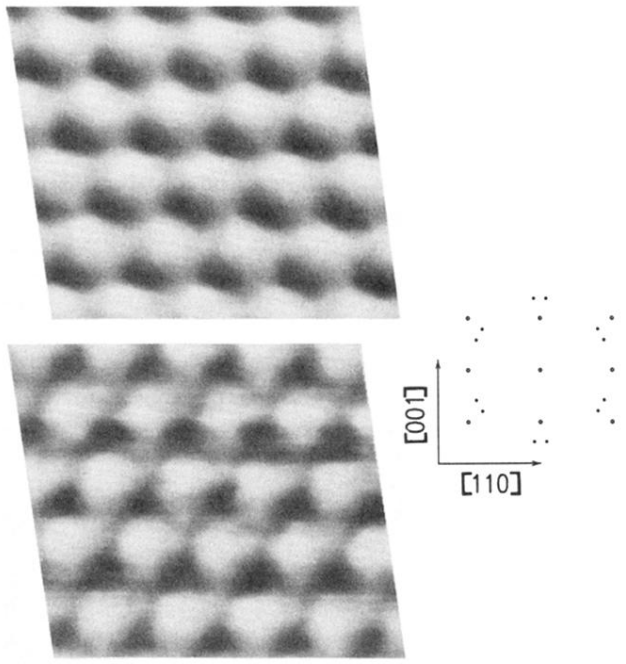

FIG. 5. Topographic images of a 20-Å × 17-Å area of a 50-Å-thick Bi film on GaP(110), at a tip current of 1 nA. Tip voltage is 0.5 eV for (a) and −1.0 eV for (b). The grey-scale range is 0.8 Å for (a) and 0.3 Å for (b). The images have been corrected for thermal drift. A schematic plot of the corresponding LEED picture is also shown, the open dots represent the substrate spots, and the solid dots come from the overlayer.